BGSG

Volume 59

Research Paper

MADAM: A Temporary Seismological Survey Experiment in Aetolia-Akarnanian Region (Western Greece)

Valentine Lefils[1,*], Alexis Rigo[1] and Efthimios Sokos[2]

[*]Laboratoire de Géologie, Ecole Normale Supérieure, PSL Research University, CNRS, 24 rue Lhomond 75005 Paris, France.
valentine.lefils@gmail.com
[1]Laboratoire de Géologie, Ecole Normale Supérieure, PSL Research University, CNRS, 24 rue Lhomond 75005 Paris, France. alexis.rigo@ens.fr
[2]Department of Geology, University of Patras, Greece. esokos@upatras.gr

Correspondence to:
Valentine Lefils
valentine.lefils@gmail.com

DOI number:
http://dx.doi.org/10.12681/bgsg.31714

Keywords:
Microseismicity, Velocity model, Western Greece

Citation:
Lefils, V., Rigo, A. and Sokos, E. (2023), MADAM: A Temporary Seismological Survey Experiment in Aetolia-Akarnanian Region (Western Greece). Bulletin Geological Society of Greece, 59, 158-174.

Publication History:
Received: 03/11/2022
Accepted: 30/12/2022
Accepted article online: 05/01/2023

The Editor wishes to thank two anonymous reviewers for their work with the scientific reviewing of the manuscript and Ms Emmanouela Konstantakopoulou for editorial assistance.

Abstract

The Aetolia-Akarnanian region, in Western Greece, is considered to be part of a micro-plate in formation, named the Ionian Island-Akarnanian Block (IAB), in the larger-scale Central Mediterranean tectonic context. The IAB accommodates the deformations between the surrounding tectonic structures that are the Corinth Gulf, the Hellenic subduction, the Kefalonia Transform Fault and the Apulian collision. This work presents the first results of a dense temporary seismic survey in the Aetolia-Akarnanian region (from the Amvrakikos Gulf to the Patras Gulf). Our local dense network has been designed in order to avoid gaps and to allow the recording of a major part of the Akarnania seismicity. With a semi-automatic events detection and picking program, we detected more than 15000 events from October 2015 to December 2018. With this important data set we constrained a 1D local velocity model. The comparison with the previous published models shows a possible significant velocity variation inside the region and especially at the Trichonis lake graben. Thanks to our data set and our velocity model, we precisely located 12723 seismic events with magnitude $0 < M_L < 4.6$, and a magnitude of completeness $Mc = 1.0$, that represents actually the most important catalogue for the Aetolia-Akarnania. Seismicity highlights specific seismic structures as clusters and a seismic plane below the West of Corinth Gulf that are briefly discussed.

Keywords: *Microseismicity, Velocity model, Western Greece.*

ΠΕΡΙΛΗΨΗ

Η περιοχή της Αιτωλοακαρνανίας, στη Δυτική Ελλάδα, θεωρείται μέρος μιας μικροπλάκας, με την ονομασία μπλοκ Ιονίων νήσων και Ακαρνανίας (Ionian Akarnanian Block, IAB). Η συγκεκριμένη μικροπλάκα συσσωρεύει την παραμόρφωση που προκαλείται από γειτονικές ενεργές δομές όπως ο Κορινθιακός κόλπος, η Ελληνική υποβύθιση, το οριζόντιο ρήγμα Κεφαλληνίας – Λευκάδας και η ζώνη σύγκρουσης της Απούλιας. Η παρούσα εργασία αναφέρεται στα πρώτα αποτελέσματα από την εγκατάσταση ενός πυκνού δικτύου σεισμογράφων στην Αιτωλοακαρνανία (από τον Αμβρακικό κόλπο έως τον Πατραϊκό). Το δίκτυο σχεδιάστηκε με τέτοιο τρόπο ώστε να καλύψει την περιοχή ομοιόμορφα και να καταγράψει τη σεισμικότητα με μεγάλη ακρίβεια. Χρησιμοποιώντας μια ημιαυτόματη διαδικασία εντοπισμού των σεισμικών γεγονότων και επιλογής των σεισμικών φάσεων, αναγνωρίστηκαν και εντοπίστηκαν περισσότερα από 15000 σεισμικά γεγονότα, για τη χρονική περίοδο, Οκτώβριος 2015 – Δεκέμβριος 2018. Με βάση τα παραπάνω δεδομένα υπολογίστηκε ένα τοπικό μοντέλο ταχυτήτων σε μια διάσταση (1D). Η σύγκριση με δημοσιευμένα μοντέλα δείχνει μια σημαντική μεταβολή της ταχύτητας στην περιοχή και κυρίως στην τάφρο της Τριχωνίδας. Χρησιμοποιώντας το ενημερωμένο μοντέλο ταχυτήτων, εντοπίστηκαν με μεγάλη ακρίβεια 12723 σεισμικά γεγονότα, με μεγέθη από $0 < M_L < 4.6$, και μέγεθος πληρότητας $Mc = 1.0$, που αποτελεί και τον πιο πλήρη σεισμικό κατάλογο για την περιοχή της Αιτωλοακαρνανίας. Στην εργασία αναλύεται η κατανομή της σεισμικότητας, η οποία εντοπίζεται σε συγκεκριμένες τεκτονικές δομές, με την μορφή συστάδων, και με τη μορφή ενός επίπεδου σεισμικού ρήγματος κάτω από το δυτικό Κορινθιακό κόλπο.

Λέξεις-Κλειδιά: *Μικροσεισμικότητα, μοντέλο ταχυτήτων, Δυτική Ελλάδα*

1. INTRODUCTION

The Ionian Island-Akarnanian Block (IAB) is a micro-plate located in the western Greece that has been recently defined by Pérouse (2013) and Pérouse et al. (2017). This micro-plate accommodates the deformation in between the Corinth Gulf (South-East), the Hellenic subduction (South), the Kefalonia Transform Fault (KTF) and the Apulian collision (West). The Hellenic subduction marks the limit between the Nubian (South) and the Anatolian (North) plates with an estimated convergence of 35 mm/yr (Nocquet, 2012) and joins the southern termination of the KTF to the West of our study area (fig.1A). The KTF is a major dextral transform fault that delimits the IAB to the west. North of the KTF, the Apulian collision against Albania and Western Greece is due to the counterclockwise rotation of the Apulian platform (Pérouse et al., 2012; D'Agostino et al., 2008). To the east of the IAB, the Corinth Gulf is one of the fastest continental

rifts in the world with between 10 to 16 mm/yr of N-S extension in its western part (Avallone et al., 2004; Briole et al., 2000; Chousianitis et al., 2013; Briole et al., 2021). The region in between, from the Patras Gulf to the south, to the Amvrakikos Gulf, to the north is characterized by a ~ North-South left lateral strike-slip fault system, the Katouna – Stamna Fault (KSF). Moreover, several East-West normal faults bordering extensional areas, as the Trichonis lake graben, the Corinth rift, the Patras Gulf and the Amvrakikos Gulf are recognized as active faults (Fig. 1B).

The National Observatory of Athens (NOA) distributes the data from the Hellenic Unified Seismic Network (HUSN, Evangelidis et al., 2021), which includes almost all the permanent seismic stations of the different Greek Universities, nearly 150 stations. With an automatic detection method and manual updating, this network locates seismic activity in the Akarnanian region. During our study time, from October 2015 to December 2018, 3187 seismic events have been located by NOA, with magnitudes ranging from 0.4 to 4.5 M_L, a magnitude of completeness at Mc = 1.8, and mean error locations at about 3.6 km.

The details of the tectonic setting and dynamics are not well resolved within the IAB, the connections with the surrounding tectonic structures are still difficult to appraise. The Aetolia-Akarnanian region is a key area to understand coexisting deformation modes due to surrounding tectonic structures. In order to better observe the seismic activity and provide geodynamical knowledge of this region, we started a seismic survey (MADAM) at the end of 2015 with a dense seismological network over the area, between the Patras Gulf and the Amvrakikos Gulf. The temporary seismic network (Fig.1B) was composed of 16 stations recording continuously at 100 Hz with short-period and enlarged short-period seismometers, and Datacube and Earthdata dataloggers to detect local seismicity. As shown in Fig. 1B, six seismometers are located to the north of Akarnania surrounding the Amvrakikos Gulf, three to the west of the KSF, and seven in the surroundings of the Trichonis lake. In addition, ten stations from the permanent networks are also used: the HUSN (HUSN Team, 2015) and the Corinth Rift Laboratory Network (CRLNET, Corinth Rift Laboratory Team and RESIF Datacenter, 2013) are composed by short-period and broad-band seismometers recording continuously at 100 Hz. Beside the temporary network, a gap in station coverage remains in the central Akarnanian region (east to the KSF) but despite this, micro-seismicity is well detected in this area (see section Seismicity and Fig. 5).

At regional scale, several seismic velocity models already exist (Hatzfeld et al., 1995; Rigo et al., 1996; Haslinger, 1998; Novotny et al., 2012; Kassaras et al., 2014, 2016)

but none of them is specifically constrained for our study area. In order to obtain precise seismic event locations and to try to characterize the local seismotectonics, we determined a new local velocity model from seismic data from October 2015 to December 2017. In this paper we present the first results of the MADAM network related to local velocity structure and seismicity distribution.

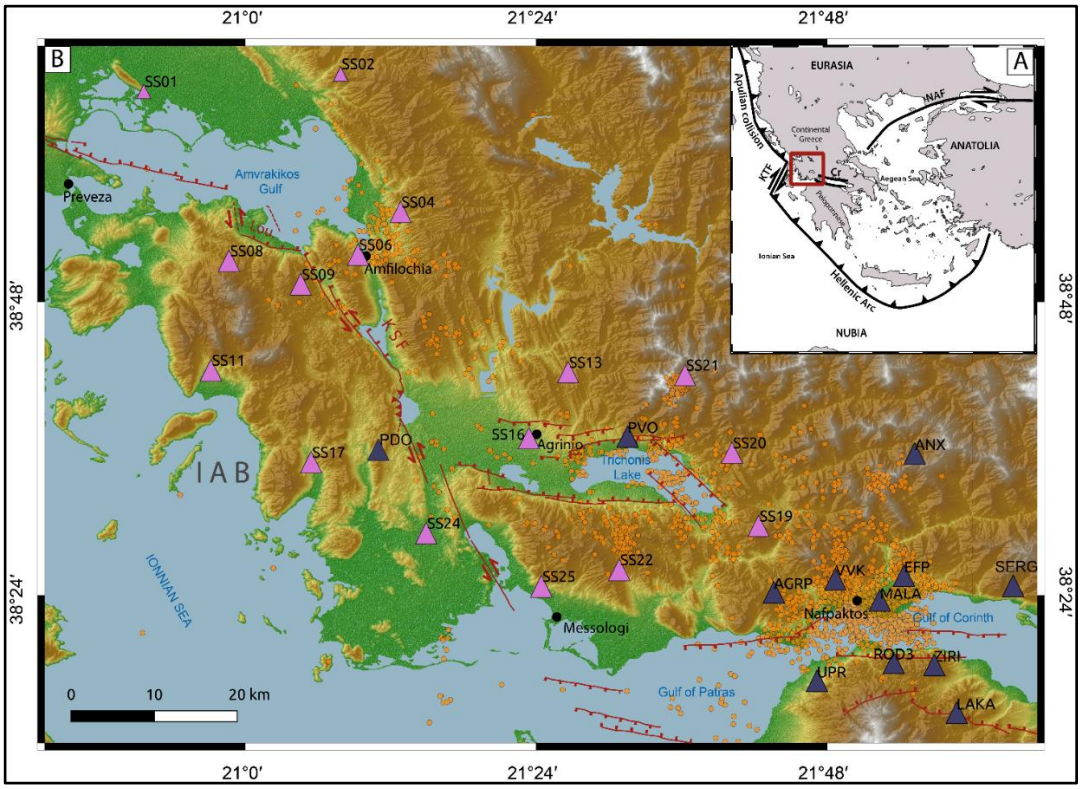

Fig. 1: Seismic networks map. A) General tectonic map, red rectangle locating the study area. B) The MADAM network corresponds to a temporary network of 16 stations (pink triangles) carried out between October 2015 and December 2018, the HUSN is the Hellenic Unified Seismic Network and the CRL is the Corinth Rift Laboratory Network (blue triangles). The seismicity used to determine the velocity model is located by orange dots. Fault traces are from Pérouse (2013) and Pérouse et al. (2017). IAB: Ionian Island Akarnanian Block, Lou: Loutraki faults, KSF: Katouna-Stamna Fault. *A high-resolution image of this figure is available online*.

2. Data Analyses

Various methods to analyze continuous seismic recordings and to detect seismic events have been proposed in the literature (e.g., Leonard and Kennett, 1999; Gentili and Michelini, 2006; Vassallo et al., 2012; Baillard et al., 2014; Bogiatzis and Ishii, 2015). One of them is based on the comparison of the mean characteristic signal over a short and a long time period to find phase time arrivals. This method using the transient increase of energy occurring during the phase arrivals, is the Short Term Average / Long Term Average method (STA/LTA) (Allen, 1978; Chen and Holland, 2016). The

STA/LTA method allows to process in a short time a huge quantity of data, but with small precision for small magnitude events due to low seismic waves amplitude generated by those events and the presence of noise. To detect a maximum number of small events recorded by the network, we developed a semi-automatic seismic detection and picking program based on the STA/LTA method. This program first applies a band-pass filter between 2.0 and 10.0 Hz. Then, it searches a transient increase of energy on continuous vertical component recordings for each seismic station using the Fbpicker function from the PhasePApy Python program (Chen and Holland, 2016). In case of a minimum of 3 stations detection in a 30-s time-window the user has to confirm the seismic event by a visual check. Then the *P*- and *S*-phases are automatically picked on each component at each station with the picker functions from Obspy (Beyreuther et al., 2010; Megies et al., 2011; Krischer et al., 2015). The last step is a visual check with possible manual corrections of phase pickings (Fig. 2). At the same time, some additional information is manually added like phases picking quality (A=good, D=bad) and *P*-wave first motion polarity (U=up, D=down). In that way, more than 15000 events were detected over the 39 months of the MADAM campaign (October 2015 - December 2018). For small amplitude events, the coda, which can be used to estimate the local magnitude M_L, was difficult to distinguish from noise, which can be significant at some stations due to anthropogenic activity. To avoid those uncertainties, we computed local magnitudes (M_L) based on the signal amplitude using the Source-Spec open source software (Satriano, 2021). The magnitude range we obtained is $0 < M_L < 4.6$ with 8 seismic events with M_L greater than 4.0: one located at Karpenisi city (NE Akarnania), one near Agrinio and the 6 others at the transition zone between Patras and Corinth gulfs (red stars in Fig. 5). According to the frequency-magnitude distribution (Gutenberg and Richter, 1944), the resulting magnitude of completeness is Mc = 1.0, with *a*-value and *b*-value at 4.90 and 0.93, respectively (Fig. 3).

Several regional seismic velocity models are already published for various parts of Western Greece (Hatzfeld et al., 1995; Rigo et al., 1996, Haslinger, 1998; Novotny et al., 2012; Kassaras et al., 2014, 2016). For the initial locations, we used the Haslinger (1998) (Fig. 4) velocity model with *hypo71* software (Lee and Lahr, 1972). The Haslinger's velocity model is the most used for the Aetolia-Akarnanian region. This model is constrained by 232 seismic events from a seismic campaign carried out in 1995, covering the northern part of the Akarnanian region (Arta-Agrinio area). This velocity model is composed of 9 layers from surface to 40 km depth corresponding to the estimated Moho depth (Hatzfeld et al., 1995; Haslinger et al., 1999), and a Vp/Vs ratio at 1.86. Nevertheless, the slow velocity (3.5 km/s *P*-wave velocity) at the most superficial layer of this model (0 – 500 m depth) is poorly constrained due to the 1D

velocity model resolution method (Haslinger, 1998), and we decided to not take it into account for our first locations.

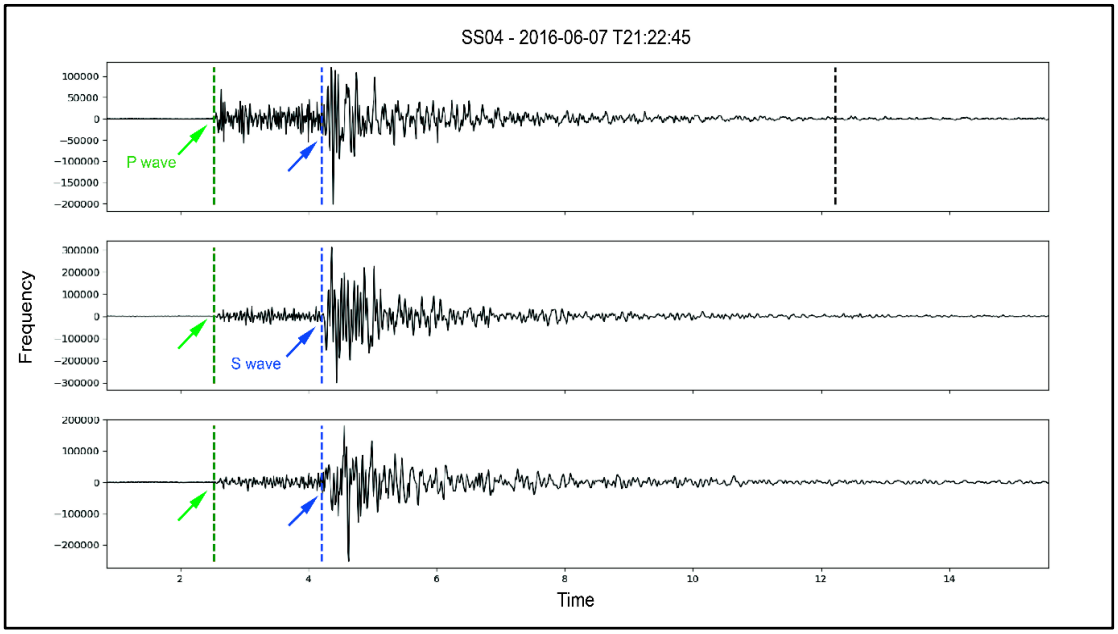

Fig. 2: *P*- and *S*-phases picking example for SS04 station. The three graphics represent the vertical, North-South and East-West components, respectively. Dashed lines depict *P*- (green), *S*- (blue) wave arrival times and event duration (coda, black).

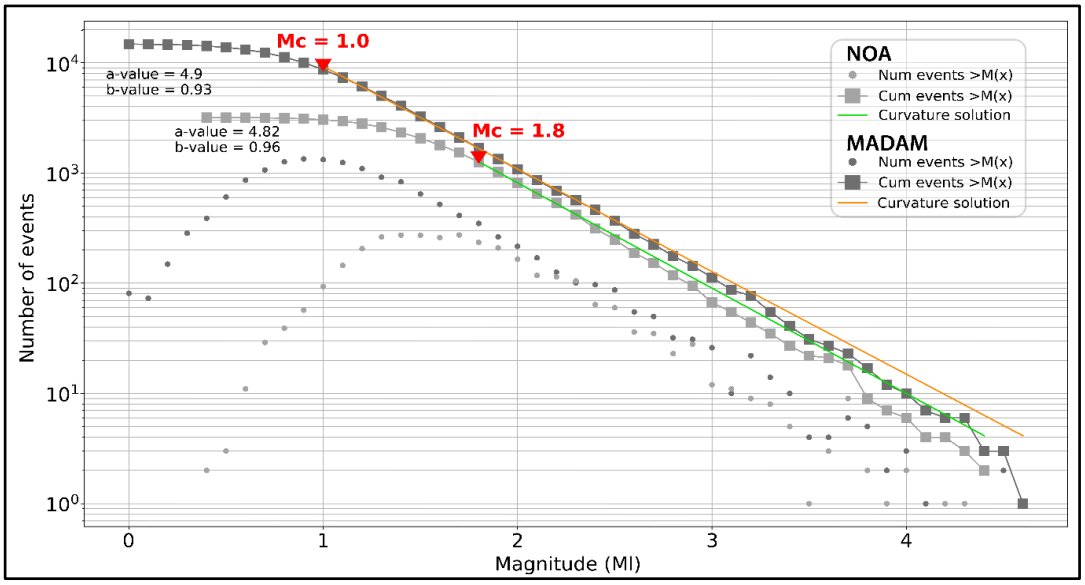

Fig. 3: Gutenberg-Richter diagram for MADAM (dark gray and orange) and NOA (light gray and green) catalogues, respectively. Number of events corresponds to circles and cumulative number of events corresponds to squares. The linear fits are curvature solution for magnitude of completeness Mc = 1.0 and Mc = 1.8 for MADAM and NOA catalogues, respectively.

3. 1-D velocity model

To improve hypocentral locations, a new velocity model for the area covered by the MADAM network and stations delays for temporal and permanent stations are

constrained from our data set using the VELEST program (Kissling et al., 1994). A total of 2343 good seismic event locations from 2015, 2016 and 2017 have been used to determine this new velocity model (Fig. 1). The good seismic event locations correspond to *hypo71* location results with the Haslinger's velocity model, and for which we obtained qualities A and B (from *hypo71* criteria), locations RMS smaller than 0.35 s, and horizontal and vertical errors smaller than 2 km and 5 km, respectively. We estimated the Vp/Vs ratio to be 1.85 from the Wadati diagram (Wadati and Oki, 1933). It agrees with the ratios obtained from previous studies in the area ranging from 1.79 to 1.86 (Hatzfeld et al., 1995; Rigo et al., 1996; Haslinger, 1998; Nocquet, 2012; Kassaras et al., 2014, 2016). The 2343 seismic events have been selected in order to be distributed over the entire study region limiting the gaps, and to constrain a velocity model on the largest tectonic structures as the Trichonis graben, the KSF strike-slip system, the West Corinth Gulf, and the Amvrakikos Gulf. The obtained 1D velocity model (red line Fig. 4) with VELEST, is composed of 8 layers from the surface to 40 km depth with *P*-wave velocities ranging from 5.40 km/s at surface to 8.04 km/s at depth (Table 1). The obtained Vp/Vs ratio at 1.84 estimated with a weighted on layers thickness is consistent with the 1.85 value found with the Wadati diagram. The robustness of this model is empirically estimated by trial-and-error calculations by changing input parameters as number and limit of layers, top layer velocity and initial velocity model. Beside those variations, these different simulations tend towards a similar result.

Table 1: 1-D P- and S-wave velocity model table with depth, P-waves velocities, S-waves velocities and the weighted mean Vp/Vs ratio obtained in our study. Moho depth is at 40 km.

Depth (km)	V_p $(km.s^{-1})$	V_s $(km.s^{-1})$	V_p/V_s
0.0	5.40	2.24	
0.5	5.45	2.71	
2.5	5.48	2.87	
5.0	6.06	3.26	
10.0	6.21	3.26	1.84
15.0	6.51	3.41	
20.0	6.75	3.82	
40.0	8.04	4.02	

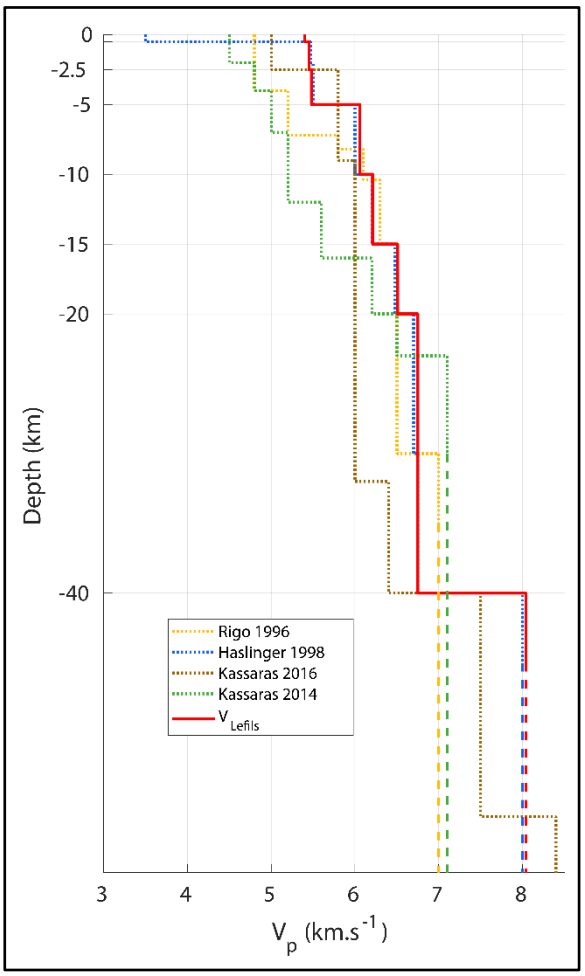

Fig. 4: 1-D *P*-wave velocity model comparison between our model, V_{Lefils} in bold red solid line (Vp/Vs = 1.84) and the previously published models : Rigo et al. (1996) (yellow dotted line) constrained for the western part of the Corinth Gulf, Vp/Vs= 1.80, Haslinger (1998) (blue dotted line) constrained for Arta-Agrinio region, Vp/Vs = 1.86, Kassaras et al. (2014) (green dotted line) constrained for the Trichonis graben, Vp/Vs = 1.79 and Kassaras et al. (2016) (brown dotted line) constrained for Akarnanian and Epirus regions, Vp/Vs = 1.83.

The objective in determining a new 1D *P*-wave velocity model was to better constrain the hypocentre locations of our big data set. Actually, no velocity model has been specifically constrained for the Akarnanian region (Amvrakikos Gulf to Corinth-Patras Gulf). The models already published have been defined for nearby area or parts of Akarnania. However, the differences in depth interfaces and *P*-velocities (Fig. 4) suggest that no models can be trusted to locate with confident precision the hypocentres. Discrepancies between the models can be explained by the differences on several parameters as the geographical zone considered, the number and the distribution of the seismological stations and the number and the location of the events used to constrain the models. Our model is close to Haslinger's model, which is the one mostly based on data covering our study area. Those similarities between those two models confirm the velocities found by Haslinger and constrain the most superficial velocity layer

consistent with crustal geology. Also, the differences between the regional and local models can not only be due to different parameterisations, but also linked to non-negligible lateral velocity variations in the area. Specifically, the differences between the model from Kassaras et al. (2014) built for a smaller area corresponding to the Trichonis graben, and the other models built for larger areas, are the most important for depths above 20 km (Fig. 4). That tends to confirm the hypothesis of strong lateral variations of *P*-wave velocities in the region.

4. Seismicity

The new 1D velocity model is used to determine more precise event locations for our data set. From the 15079 detected events, thanks to *hypo71* and using stations delays determined with VELEST, we have been able to precisely locate 12723 events with mean vertical errors of 3.2 km, mean horizontal errors of 0.8 km, and a mean RMS of 0.26 s (Fig. 5). The seismicity is well distributed all over the region and mostly restricted between the surface and 30 km depth, with magnitudes M_L ranging from 0 to 4.6. This catalogue is actually the most complete catalogue for the Akarnanian region. If we compare to the NOA catalogue, it has 4 times more events that have been located for the same region and same time period (3187 events for NOA against 12723 events for MADAM). The difference in the magnitudes of completeness, i.e., Mc = 1.8 for NOA and Mc = 1.0 for MADAM catalogue, highlights the accuracy of the MADAM catalogue compared to the NOA one (Fig. 3). The new velocity model used (Table 1) compared to the Greek global velocity model used by NOA for hypocentre locations gives a shallower seismicity, with depths mostly between surface to 30 km for the MADAM catalogue compared to surface to 40 km depth for the NOA catalogue.

In addition, the obtained precise locations, bring information about locations, origins and type of structures of the seismogenic active zones of the Aetolia-Akarnanian region. On first approach, the relationship between active faults and seismicity is not obvious (Fig. 5). For sure, on most normal faults (West Corinth Gulf and Trichonis graben) there is a clear intense seismic activity. On the contrary, the seismicity is less important on the Loutraki and Patras Gulf normal faults, and on most parts of the KSF. Nevertheless, seismic activity on the KSF seems to be located on relay zones, between the Katouna and the Stamna faults to the south, and on Katouna geometric direction changes to the north. Also, intense seismic activity stands out from zones without any known mapped active faults like in Messologi bay, to the south of the Amvrakikos Gulf (between SS08 and SS11 seismic stations) or to the north and the south out of Trichonis lake. The event distribution in the region is non-homogeneous and shows important dense seismic zones. As examples, high seismic density is clearly apparent to the north of the

Trichonis graben around 10 km depth (Fig. 5B) and also to the South-West in Messologi bay (at 21°17'E, 38°20'N on map, Fig. 5A). The temporal evolution of the seismicity (Fig. 6) indicates that these dense seismic activities are not only spatial (from few events to several hundred events) but also temporal (from some days to several tens of days). Those one-off increases of the seismicity are spatio-temporal clusters. Likewise, another specific seismic structure already observed in previous studies (Rigo et al., 1996; Godano et al., 2014; Lambotte et al., 2014; Duverger et al., 2018; Kaviris et al., 2021) is highlighted in the western Corinth Gulf (Fig. 5A). This big structure encompasses more than 50% of the MADAM catalogue seismicity. The West Corinth Gulf stands out by a seismic plane with about 30 km radius around Nafpaktos city. This plane is dipping between 5° and 30° to the North between 5 and 25 km depth (Fig. 5B) from South of the Corinth rift to East of the Trichonis graben (Fig. 5A). Compared to clusters, this plane differs not only by its size, but also by its temporal evolution being continuously active during the time of observation.

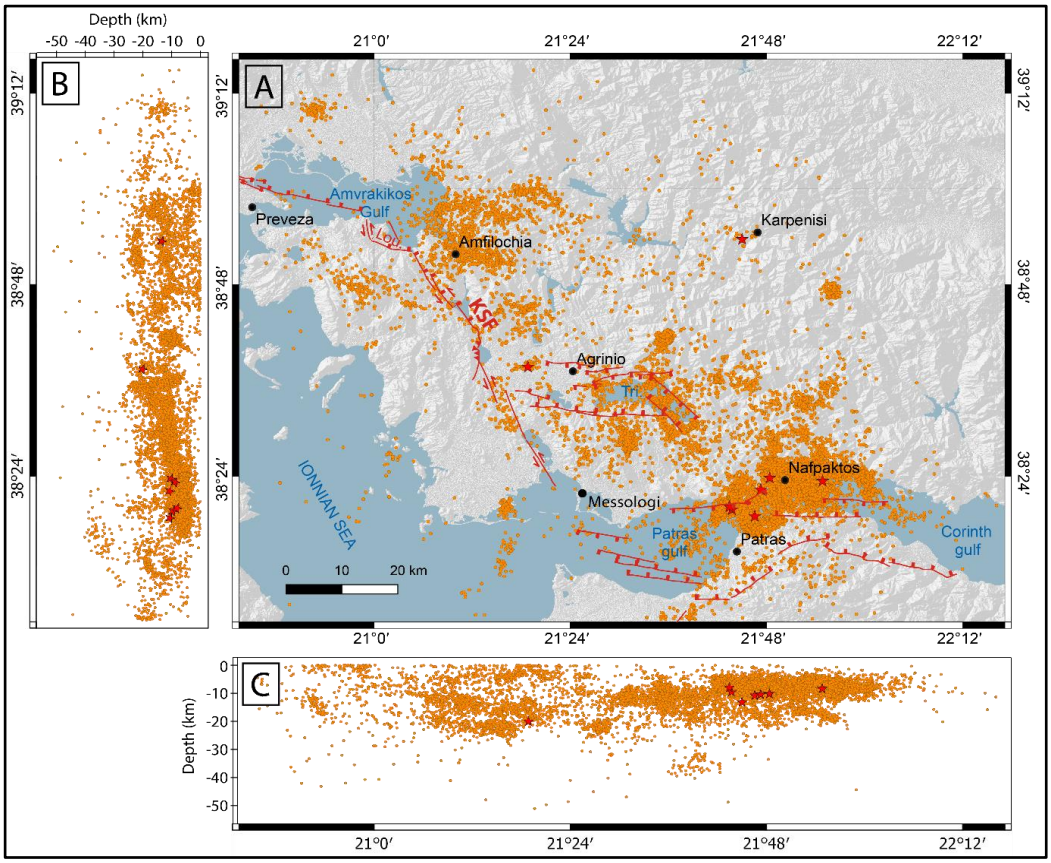

Fig. 5: Located seismic events map from the MADAM catalogue. The locations are from *hypo71* software (Lee and Lahr, 1972) with the new velocity model considering stations delays from VELEST. Red stars correspond to M_L > 4.0 and red traces correspond to fault traces from Pérouse (2013) and Pérouse et al. (2017). A) Seismicity map, B) N-S vertical cross-sections with projections of all seismic events, C) E-W vertical cross-sections with projections of all seismic events. *A high-resolution image of this figure is available online*.

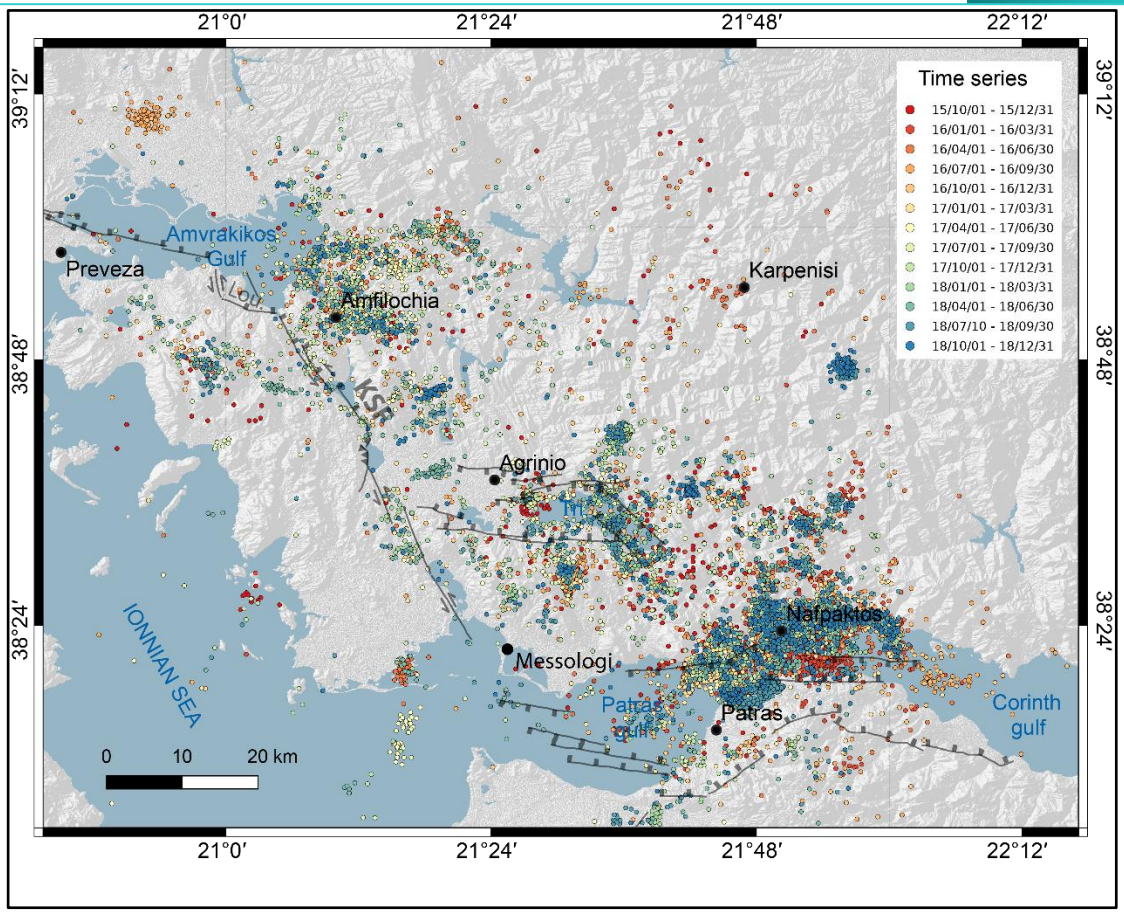

Fig. 6: Temporal evolution map of the seismicity from the MADAM catalogue. Each colour corresponds to one trimester from October 2015 to December 2018. Black traces correspond to fault traces from Pérouse (2013) and Pérouse et al. (2017). *A high-resolution image of this figure is available online*.

5. Conclusions

The seismicity of the Aetolia-Akarnanian region was recorded from October 2015 to December 2018 with good seismic detectability thanks to the MADAM seismic campaign. The huge quantity of data is processed with a semi-automatic detection and picking python program. Due to the good spatial distribution of the seismic stations and the data set, we can provide a new 1D velocity model constrained for the entire Akarnania (from Amvrakikos Gulf to West Corinth Gulf). The comparison of velocities and model coverage with previously published velocity models from the same area suggests that there must be a non-negligible lateral variation of the crustal seismic wave velocities particularly at the Trichonis graben. The 12723 well located seismic events are the most complete seismic catalogue of the Akarnania with 4 times more events than NOA catalogue over the same period.

The major KSF strike-slip fault is poorly seismically active, except on geometric direction changes. Whereas, on the Trichonis graben, West Corinth Gulf and at the East of Amvrakikos Gulf the seismic activity is important as these areas are characterised by

the presence of important active tectonic structures. There is evidence of the presence of seismicity clusters by a non-homogeneous seismic distribution and several one-off increases in the temporal distribution. A seismic plane continuously seismically active at the western termination of the Corinth Gulf is highlighted by the MADAM catalogue. This plane, already observed in previous studies (Duverger et al., 2018; Kaviris et al., 2021) is gently dipping to the north from Corinth rift to east of the Trichonis lake graben. This is the first time that this plane is seen as far to the north and in depth (25 km depth). Specific structures like clusters and a large-scale seismic plane reveal the details of the physical processes that could impact the region. In a second step, additional analyses of the seismicity as relocations, spatio-temporal evolutions or focal mechanisms will provide new information to understand deformation and seismotectonic pattern in the Akarnanian region and possibly will help to build a seismotectonic model consistent with the regional geodynamics.

6. Data and Resources

Seismic data and seismograms from HUSN network are available online on the National Observatory of Athens website https://www.gein.noa.gr/en/services-products/database-search/. Seismograms from CRL network is available online on the Résif website https://seismology.resif.fr/networks/\#/CL. Seismograms were collected using the temporary MADAM network, available on request to A. RIGO (rigo@geologie.ens.fr). Topography is from SRTM 30 m files available online on the USGS website https://earthexplorer.usgs.gov/.

7. Acknowledgments

This work benefited from the support of CNRS/INSU Tellus/Aleas 2016 and 2017. E.S. acknowledges financial support by the HELPOS project, "*Hellenic Plate Observing System" (MIS 5002697*). We thank George Andriopoulos, Nicos Germenis, Dimitri Giannopoulos, Paris Paraskevopoulos, and Christos Evangelidis for their help in the field and with the instruments, and Hélène Lyon-Caen for her help in the magnitude determinations.

8. References

Allen, R. V., 1978. Automatic earthquake recognition and timing from single traces. *Bulletin of the seismological society of America*, 68 (5), 1521–1532, https://doi.org/10.1785/BSSA0680051521.

Avallone, A., Briole, P., Agatza-Balodimou, A. M., Billiris, H., Charade, O., Mitsakaki, C., Nercessian, A., Papazissi, K., Paradissis, D., and Veis, G., 2004. Analyse de onze années de mesures de deformations collectées par GPS dans la zone du laboratoire du rift de Corinthe. Comptes Rendus. *Geoscience*, 336, 301-311. https://doi.org/10.1016/J.CRTE.2003.12.007

Baillard, C., Crawford, W. C., Ballu, V., Hibert, C., and Mangeney, A., 2014. An automatic kurtosis-based p-and s-phase picker designed for local seismic networks. *Bulletin of the Seismological Society of America*, 104, 394–409. https://doi.org/10.1785/0120120347.

Beyreuther, M., Barsch, R., Krischer, L., Megies, T., Behr, Y., and Wassermann, J., 2010. Obspy: A python toolbox for seismology. *Seismological Research Letters*, 81 (3), 530–533. https://doi.org/10.1785/GSSRL.81.3.530.

Bogiatzis, P. and Ishii, M., 2015. Continuous wavelet decomposition algorithms for automatic detection of compressional-and shear-wave arrival times. *Bulletin of the Seismological Society of America*, 105 (3), 1628–1641. https://doi.org/10.1785/0120140267.

Briole, P., Rigo, A., Lyon-Caen, H., Ruegg, J. C., Papazissi, K., Mitsakaki, C., Balodimou, A., Veis, G., Hatzfeld, D., and Deschamps, A., 2000. Active deformation of the Corinth rift, Greece: Results from repeated global positioning system surveys between 1990 and 1995. *Journal of Geophysical Research: Solid Earth*, 105, 25605–25625. https://doi.org/10.1029/2000JB900148.

Briole, P., Ganas, A., Elias, P., and Dimitrov, D., 2021. The GPS velocity field of the Aegean. new observations, contribution of the earthquakes, crustal blocks model. *Geophysical Journal International*, 226 (1), 468–492. https://doi.org/10.1093/GJI/GGAB089.

Chen, C. and Holland, A. A., 2016. Phasepapy: A robust pure python package for automatic identification of seismic phases. *Seismological Research Letters*, 87, 1384–1396, https://doi.org/10.1785/0220160019.

Chousianitis, K., Ganas, A., and Gianniou, M., 2013. Kinematic interpretation of present-day crustal deformation in central Greece from continuous GPS measurements. *Journal of Geodynamics*, 71, 1–13. https://doi.org/10.1016/J.JOG.2013.06.004.

Corinth Rift Laboratory Team and RESIF Datacenter, 2013. Cl - Corinth rift laboratory seismological network (crlnet). resif - réseau sismologique et géodésique français.

D'Agostino, N., Avallone, A., Cheloni, D., D'Anastasio, E., Mantenuto, S., and Selvaggi, G., 2008. Active tectonics of the Adriatic region from GPS and earthquake slip vectors. *Journal of Geophysical Research: Solid Earth*, 113. https://doi.org/10.1029/2008JB005860.

Duverger, C., 2017. Sismicité, couplages sismique-asismiques et processus transitoires de déformation dans un système de failles actives: le rift de Corinthe, Grèce. https://theses.hal.science/tel-02151611

Duverger, C., Lambotte, S., Bernard, P., Lyon-Caen, H., Deschamps, A., and Nercessian, A., 2018. Dynamics of microseismicity and its relationship with the active structures in the western Corinth rift (Greece). *Geophysical Journal International*, 215, 196–221. https://doi.org/10.1093/gji/ggy264.

Evangelidis, C. P., Triantafyllis, N., Samios, M., Boukouras, K., Kontakos, K., Ktenidou, O.-J., Fountoulakis, I., Kalogeras, I., Melis, N. S., Galanis, O., et al. 2021. Seismic waveform data from Greece and Cyprus: Integration, archival, and open access. *Seismological Society of America*, 92 (3), 1672–1684. https://doi.org/10.1785/0220200408.

Gentili, S. and Michelini, A., 2006. Automatic picking of p and s phases using a neural tree. *Journal of Seismology*, 10 (1), 39–63. https://doi.org/10.1007/s10950-006-2296-6.

Godano, M., Deschamps, A., Lambotte, S., Lyon-Caen, H., Bernard, P., and Pacchiani, F., 2014. Focal mechanisms of earthquake multiplets in the western part of the Corinth rift (Greece): Influence of the velocity model and constraints on the geometry of the active faults. *Geophysical Journal International*, 197, 1660–1680. https://doi.org/10.1007/s10950-006-2296-6.

Gutenberg, B. and Richter, C. F., 1944. Frequency of earthquakes in California. *Bulletin of the Seismological society of America*, 34 (4), 185–188. https://doi.org/10.1785/BSSA0340040185.

Haslinger, F., 1998. Velocity structure, seismicity and seismotectonics of northwestern Greece between the gulf of Arta and Zakynthos. https://doi.org/10.3929/ethz-a-002025706

Haslinger, F., Kissling, E., Ansorge, J., Hatzfeld, D., Papadimitriou, E., Karakostas, V., Makropoulos, K., Kahle, H.-G., and Peter, Y., 1999. 3D crustal structure from local earthquake tomography around the gulf of Arta (Ionian region, NW Greece). *Tectonophysics*, 304, 201–218. https://doi.org/10.1016/S0040-1951(98)00298-4.

Hatzfeld, D., Kassaras, I., Panagiotopoulos, D., Amorese, D., Makropoulos, K., Karakaisis, G., and Coutant, O., 1995. Microseismicity and strain pattern in northwestern Greece. *Tectonics*, 14, 773–785. https://doi.org/10.1029/95TC00839.

HUSN Team 2005. H.U.S.N - Hellenic unified seismic network. https://www.gein.noa.gr/en/networks-equipment/hellenic-unified-seismic-network-h-u-s-n/.

Kassaras, I., Kapetanidis, V., and Karakonstantis, A., 2016. On the spatial distribution of seismicity and the 3d tectonic stress field in western Greece. *Physics and Chemistry of the Earth*, 95, 50–72. https://doi.org/10.1016/j.pce.2016.03.012.

Kassaras, I., Kapetanidis, V., Karakonstantis, A., Kaviris, G., Papadimitriou, P., Voulgaris, N., Makropoulos, K., Popandopoulos, G., and Moshou, A., 2014. The April-June 2007 Trichonis lake earthquake swarm (w. Greece): New implications toward the causative fault zone. *Journal of Geodynamics*, 73, 60–80. https://doi.org/10.1016/j.jog.2013.09.004.

Kaviris, G., Elias, P., Kapetanidis, V., Serpetsidaki, A., Karakonstantis, A., Plicka, V., Barros, L. D., Sokos, E., Kassaras, I., Sakkas, V., Spingos, I., Lambotte, S., Duverger, C., Lengliné, O., Evangelidis, C. P., Fountoulakis, I., Ktenidou, O.-J., Gallovič, F., Bufféral, S., Klein, E., Aissaoui, E. M., Scotti, O., Lyon-Caen, H., Rigo, A., Papadimitriou, P., Voulgaris, N., Zahradnik, J., Deschamps, A., Briole, P., and Bernard, P., 2021. The western gulf of Corinth (Greece) 2020-2021 seismic crisis and cascading events: First results from the Corinth rift laboratory network. *The Seismic Record*, 1, 85–95. https://doi.org/10.1785/0320210021.

Kissling, E., Ellsworth, W. L., Eberhart-Phillips, D., and Kradolfer, U., 1994. Initial reference models in local earthquake tomography. *Journal of Geophysical Research*, 99. https://doi.org/10.1029/93JB03138.

Krischer, L., Megies, T., Barsch, R., Beyreuther, M., Lecocq, T., Caudron, C., and Wassermann, J. 2015. Obspy: A bridge for seismology into the scientific python ecosystem. *Computational Science & Discovery*, 8 (1), 014003. https://doi.org/10.1088/1749-4699/8/1/014003.

Lambotte, S., Lyon-Caen, H., Bernard, P., Deschamps, A., Patau, G., Nercessian, A., Pacchiani, F., Bourouis, S., Drilleau, M., and Adamova, P., 2014. Reassessment of the rifting process in the western Corinth rift from relocated seismicity. *Geophysical Journal International*, 197, 1822–1844. https://doi.org/10.1093/GJI/GGU096.

Lee, W. H. K. and Lahr, J. C., 1972. HYPO71: A computer program for determining hypocenter, magnitude, and first motion pattern of local earthquakes. US Department of the Interior, Geological Survey, National Center for Earthquake Research. https://doi.org/10.3133/OFR75311.

Leonard, M. and Kennett, B., 1999. Multi-component autoregressive techniques for the analysis of seismograms. *Physics of the Earth and Planetary Interiors*, 113 (1-4), 247–263. https://doi.org/10.1016/S0031-9201(99)00054-0.

Megies, T., Beyreuther, M., Barsch, R., Krischer, L., and Wassermann, J., 2011. Obspy–what can it do for data centers and observatories? *Annals of Geophysics*, 54 (1), 47–58. https://doi.org/10.4401/AG-4838 .

Nocquet, J. M., 2012. Present-day kinematics of the Mediterranean: A comprehensive overview of GPS results. *Tectonophysics*, 579, 220–242. https://doi.org/10.1016/j.tecto.2012.03.037.

Novotný, O., Sokos, E., and Plicka, V., 2012. Upper crustal structure of the western Corinth gulf, Greece, inferred from arrival times of the January 2010 earthquake sequence. *Studia Geophysica et Geodaetica*, 56, 1007–1018. https://doi.org/10.1007/s11200-011-0482-7.

Pérouse, E., 2013. Cinématique et tectonique active de l'Ouest de la Grèce dans le cadre géodynamique de la Méditerranée Centrale et Orientale. https://theses.hal.science/tel-00842274

Pérouse, E., Chamot-Rooke, N., Rabaute, A., Briole, P., Jouanne, F., Georgiev, I., and Dimitrov, D., 2012. Bridging onshore and offshore present-day kinematics of central and eastern Mediterranean: Implications for crustal dynamics and mantle flow. *Geochemistry, Geophysics, Geosystems*, 13. https://doi.org/10.1029/2012gc004289.

Pérouse, E., Sébrier, M., Braucher, R., Chamot-Rooke, N., Bourlès, D., Briole, P., Sorel, D., Dimitrov, D., and Arsenikos, S., 2017. Transition from collision to subduction in western Greece: the Katouna–Stamna active fault system and regional kinematics. *International Journal of Earth Sciences*, 106, 967–989. https://doi.org/10.1007/s00531-016-1345-9.

Rigo, A., Lyon-Caen, H., Armijo, R., Deschamps, A., Hatzfeld, D., Makropoulos, K., Papadimitriou, P., and Kassaras, I., 1996. A microseismic study in the western part of the gulf of Corinth (Greece): Implications for large-scale normal faulting mechanisms, *Geophysical Journal International*, 126, 663–688. https://doi.org/10.1111/J.1365-246X.1996.TB04697.X.

Satriano, C., 2021. Sourcespec – earthquake source parameters from P- or S-wave displacement spectra. https://doi.org/10.5281/ZENODO.3688587.

Vassallo, M., Satriano, C., and Lomax, A., 2012. Automatic picker developments and optimization: A strategy for improving the performances of automatic phase pickers. *Seismological Research Letters*, 83 (3), 541. https://doi.org/10.1785/gssrl.83.3.541

Wadati, K. and Oki, S., 1933. On the travel time of earthquake waves, ii, *Geophys. Mag*, 7, 101–111. https://doi.org/10.2151/jmsj1923.11.1_14 .